Coherence Attribute Applications on Seismic Data in Various Guises*

Satinder Chopra[1] and Kurt J. Marfurt[2]

Search and Discovery Article #42273 (2018)**
Posted September 17, 2018

*Adapted from oral presentation given at 2018 AAPG Annual Convention & Exhibition, Salt Lake City, Utah, May 20-23, 2018
 DOI:10.1306/42273Chopra2018

[1]TGS, Calgary, Canada (schopra@arcis.com)
[2]University of Oklahoma, Norman, Oklahoma, USA

Abstract

The iconic coherence attribute is very useful for geologic feature imaging such as faults, deltas, submarine canyons, karst collapse, mass transport complexes, and more. Besides its preconditioning, the interpretation of discrete stratigraphic features on seismic data is also limited by its bandwidth, where in general the data with higher bandwidth yields crisper features than data with lower bandwidth. Some form of spectral balancing applied to the seismic amplitude data can help in achieving such an objective, so that coherence run on spectrally balanced seismic data yields a better definition of the geologic features of interest. The quality of the generated coherence attribute is also dependent in part on the algorithm employed for its computation. In the eigenstructure decomposition procedure for coherence computation, spectral balancing equalizes each contribution to the covariance matrix, and thus yields crisper features on coherence displays. There are other ways to *modify the spectrum of the input data* in addition to simple spectral balancing, including the amplitude-volume technique (AVT), taking the derivative of the input amplitude, spectral bluing, and thin-bed spectral inversion. We compare some of those techniques, and show their added value in seismic interpretation.

We run energy ratio coherence on input seismic data, and a number of other versions that we generate in terms of voice components obtained by using continuous wavelet transform method of spectral decomposition, spectral balanced version obtained by using thin-bed reflectivity inversion, and AVT attributes. Our comparison of the equivalent time slice displays from the coherence volumes allows us to infer, (a) coherence on spectrally balanced input seismic data yields better lineament detail, (b) coherence on voice components highlights the discontinuities at different frequencies that show better definition, which can be helpful for their interpretation, (c) multispectral coherence displays show crisper definition of lineaments and so are useful, (d) coherence run on the versions of the data discussed above after AVT shows superior definition of lineaments and hence we recommend should be used in their interpretation.

References Cited

Bahorich, M.S., and S.L. Farmer, 1995, 3-D seismic coherency for faults and stratigraphic features: The Leading Edge, v. 14, p. 1053-1058.

Bakker, P., 2003, Image structure analysis for seismic interpretation: Ph.D. Thesis, Technische Universiteit Delft.

Chopra, S., V. Sudhakar, G. Larsen, and H. Leong, 2000, Azimuth based coherence for detecting faults and fractures: World Oil, v. 21, September, p. 57-62.

Chopra, S., and K.J. Marfurt, 2008, Gleaning meaningful information from seismic attributes: First Break, v. 26, p. 43-53.

Gersztenkorn, A., and K.J. Marfurt, 1999, Eigenstructure-basd coherence computations as an aid to 3D structural and stratigraphic mapping: Geophysics, v. 64, p. 1468-1479.

Marfurt, K.J., R.L. Kirlin, S.H. Farmer, and M.S. Bahorich, 1998, 3-D seismic attributes using a running window semblance-based algorithm: Geophysics, v. 63, p. 1150-1165.

Marfurt, K.J., 2017, Interpretational aspects of multispectral coherence: 79th Annual EAGE Conference and Exposition, Expanded Abstract, Th A4 11.

Pepper, R., and G. Bejarano, 2005, Advances in seismic fault interpretation automation: AAPG/Datapages Search and Discovery article #40169. Website accessed September 5, 2018.
http://www.searchanddiscovery.com/pdfz/documents/2005/pepper/images/pepper.pdf.html

Qi, J., F. Li, and K.J. Marfurt, 2017, Multiazimuth coherence: Geophysics, v. 82/6, PO83-O89.

Coherence attribute applications on seismic data in various guises

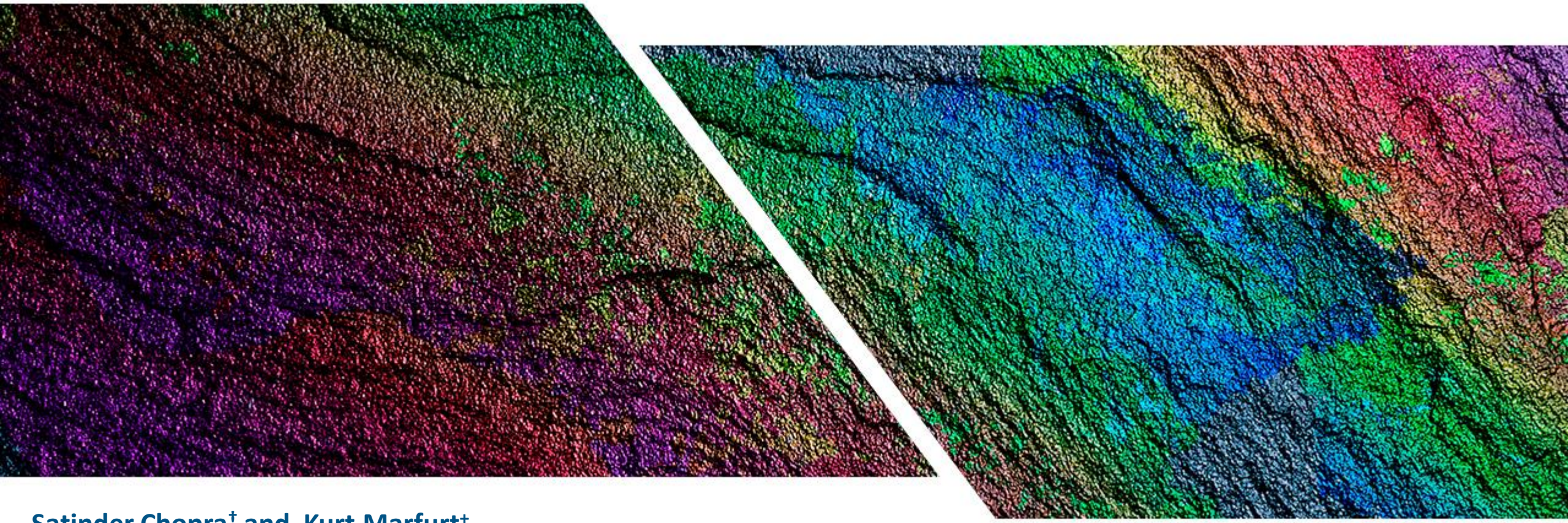

Satinder Chopra[†] and Kurt Marfurt[+]

[†]TGS, Calgary; [+]The University of Oklahoma, Norman

Talk delivered at AAPG Convention, Salt Lake City on 21st May, 2018

Coherence attribute

- Iconic discontinuity attribute
- Available on most interpretation workstation software packages
- Often used along with curvature and other attributes using transparency
- Useful attribute

Coherence attribute

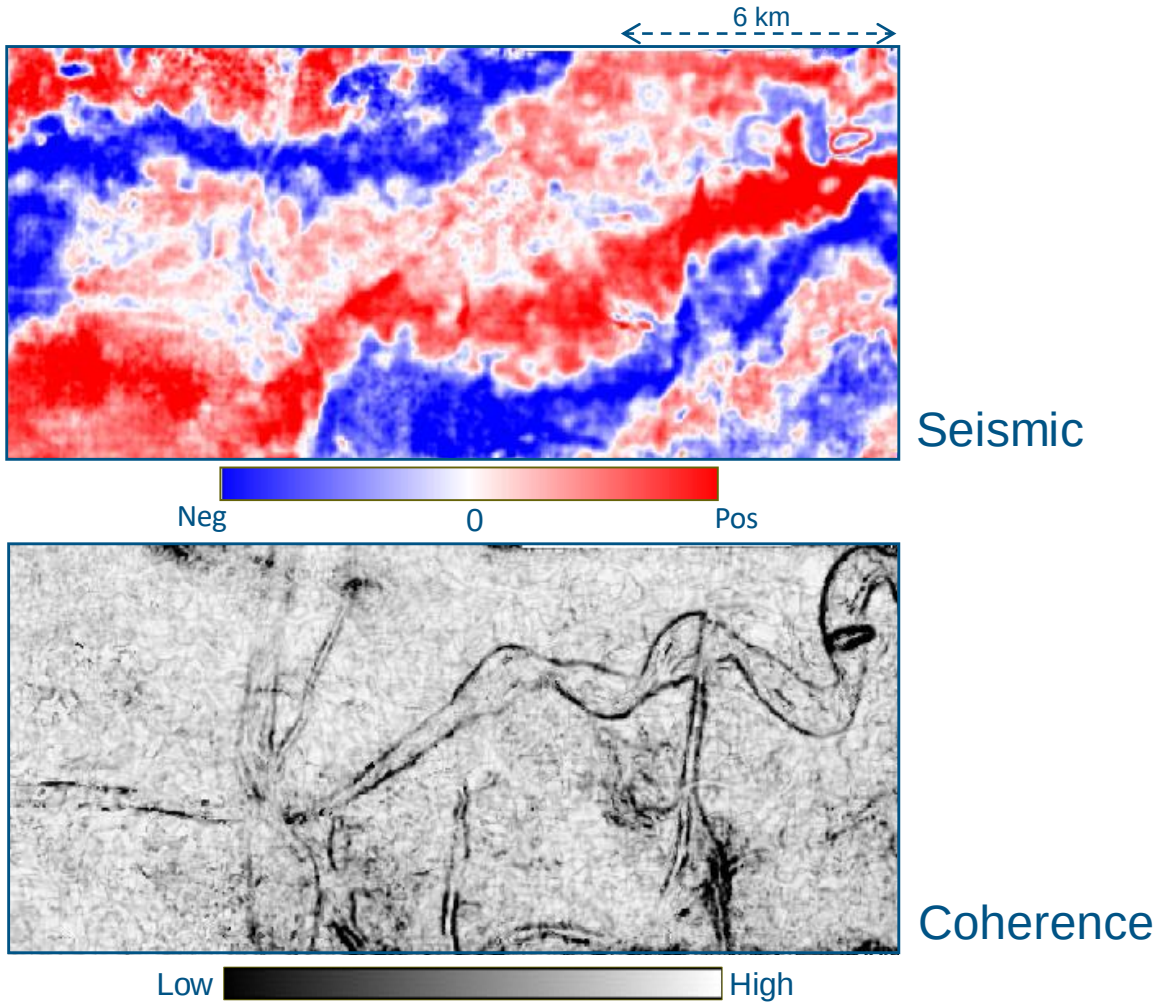

Equivalent horizon slices from (above) seismic, and (below) coherence volumes. The definition of different channels seen on the coherence display is difficult to detect on the seismic display.

Coherence attribute

Different algorithms have evolved over time

- Crosscorrelation-based (*Bahorich and Farmer, 1995*)
- Semblance-based (*Marfurt et al., 1998*)
- Variance-based (*Pepper and Bejarano, 2005*)
- Eigen-decomposition-based (*Gersztenkorn and Marfurt, 1999*)
- Gradient structure tensor-based (*Bakker, 2003*)
- Energy ratio-based (*Chopra and Marfurt, 2008*)

Coherence attribute

On input seismic

On input seismic with spectral enhancement

Low High

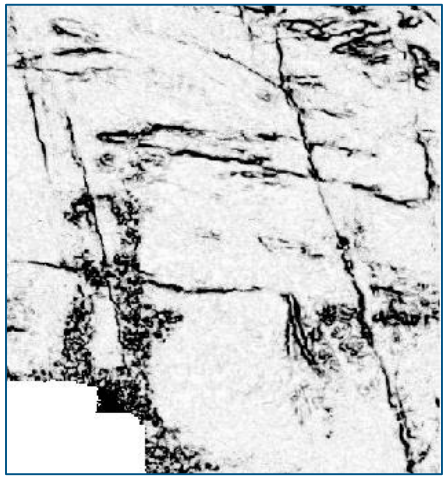

On voice component (65 Hz)

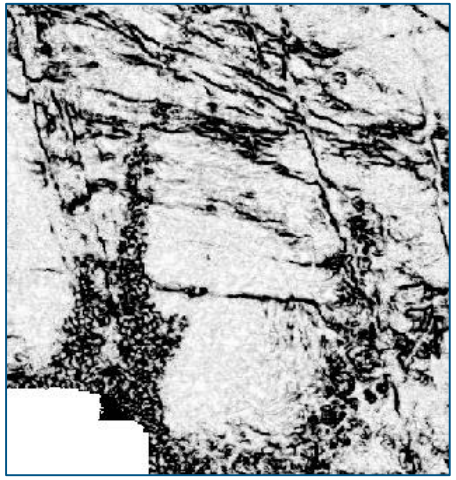

On voice component (75 Hz)

On voice component (85 Hz)

Time slices at 1322 ms, from the coherence attribute run on different volumes

Voice components

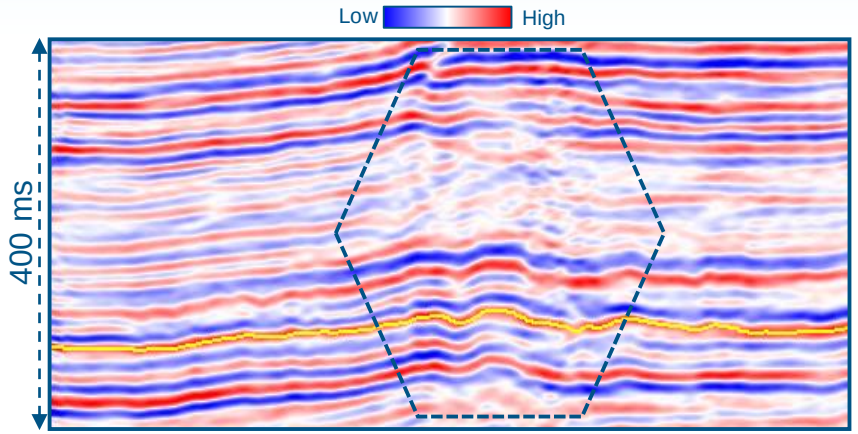

Seismic

b)

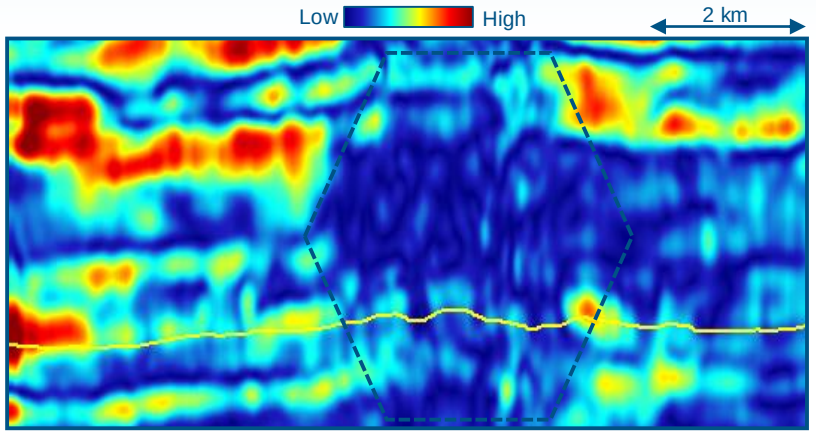

Spectral magnitude

c)

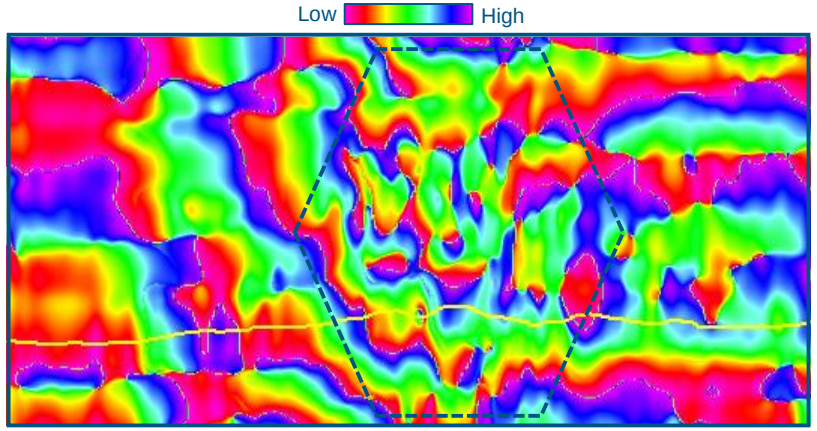

Spectral phase

d)

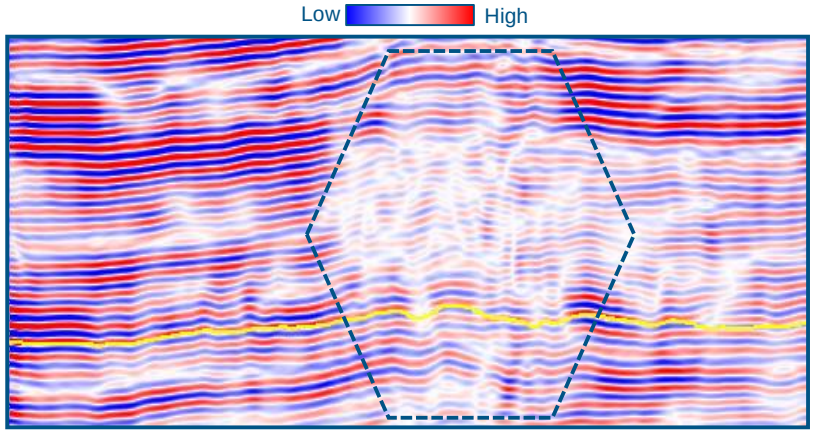

Voice component (65 Hz)

Notice the vertical discontinuities in the highlighted portion are poorly seen in the original broadband data, are not seen in the spectral magnitude component, but are clearly seen in the spectral phase and voice components. The voice component has the advantage that it can be easily interpreted and processed (e.g. using coherence) as one would the original seismic amplitude data.

Spectral decomposition

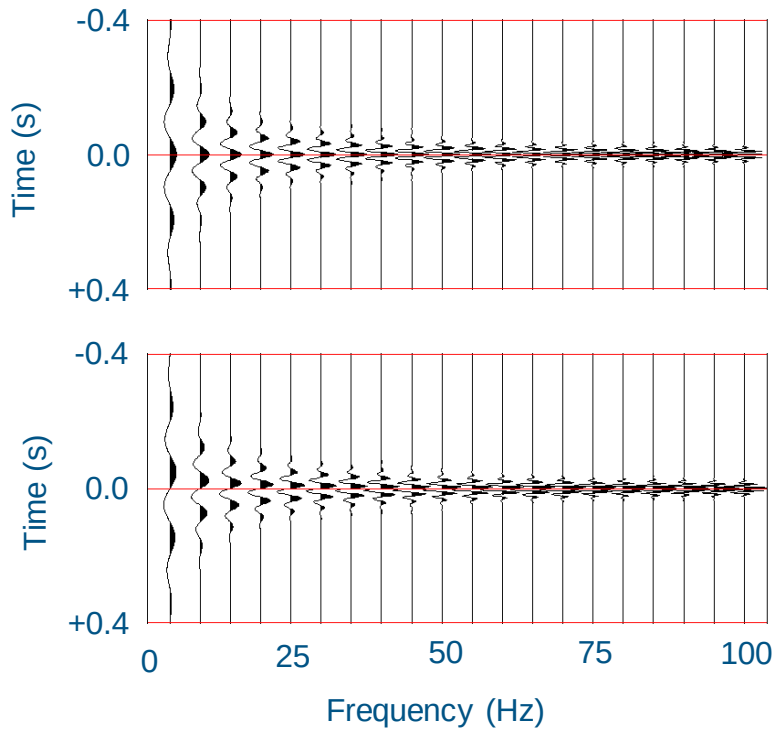

Complex wavelets used in the continuous wavelet transform. The (top) real and (bottom) imaginary (or 90^0-phase rotated) wavelets are simply convolved with the input seismic trace about each sample to form $v(t,f)$ and $v^H(t,f)$. The convolution with the real wavelets provides the voices, $v(t,f)$.

The spectral magnitude, $a(t,f)$, is defined as $m(t,f)=\{[v(t,f)]^2+[v^H(t,f)]^2\}^{1/2}$

Picking horizons using voice components

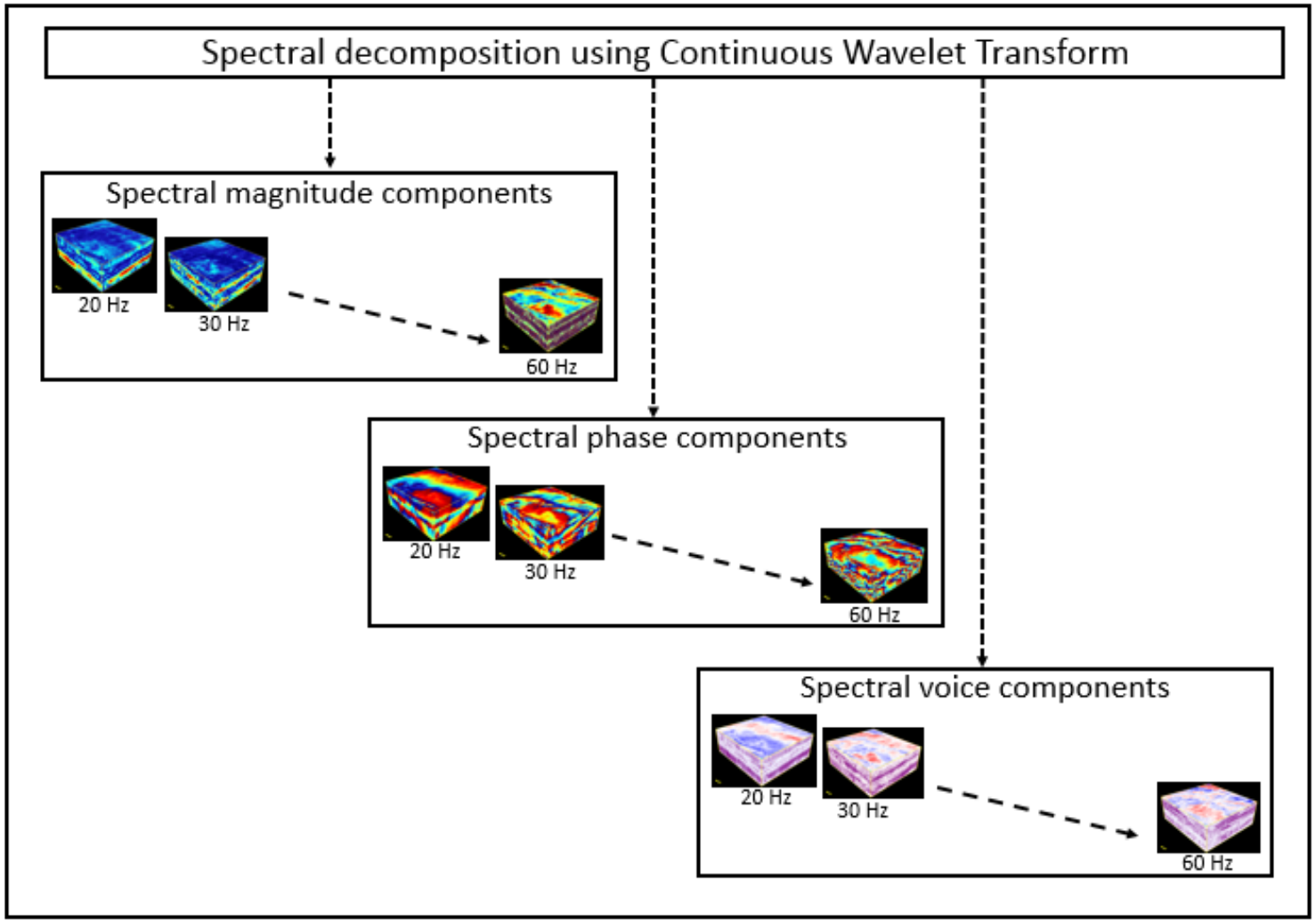

Typical workflow for spectral decomposition carried out using the continuous wavelet transform method. The output includes spectral magnitude, phase, and voice component volumes.

Spectral decomposition

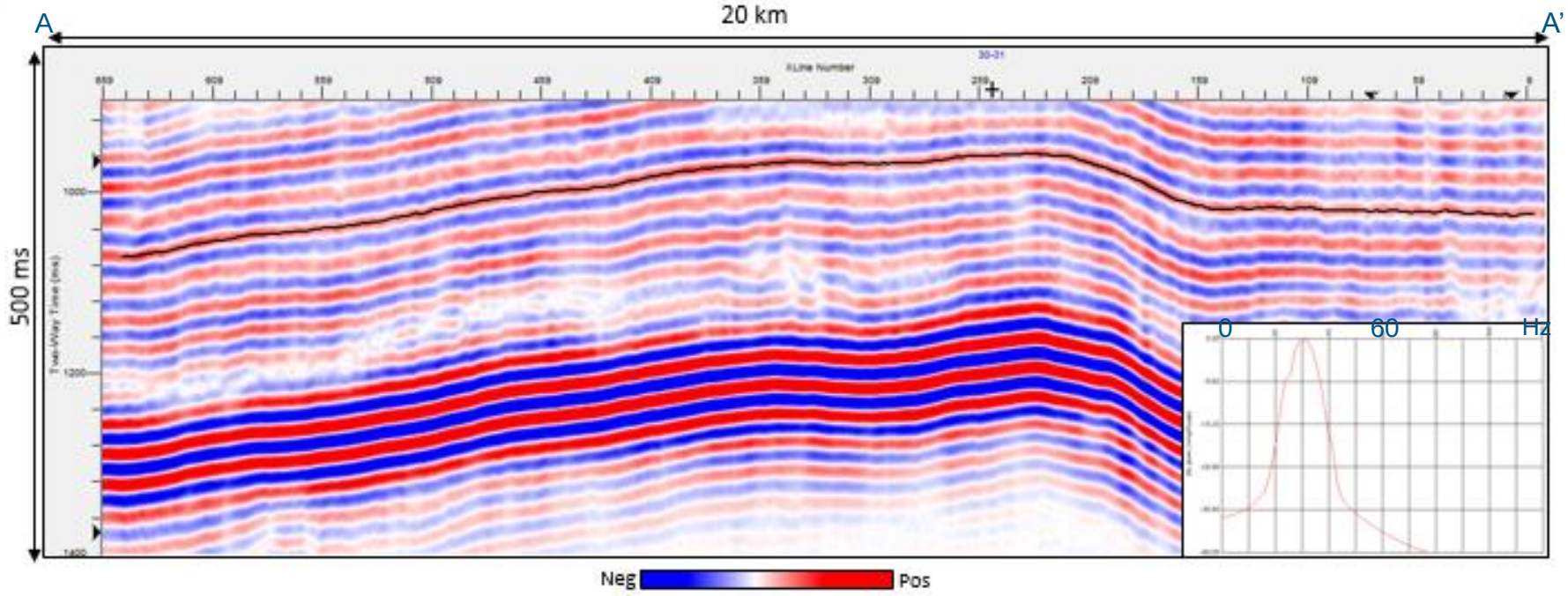

A vertical slice through the 30 Hz voice component after spectral decomposition with spectral balancing and its amplitude spectrum. Notice the frequency width on both sides of the amplitude maxima seen at 30 Hz. (*Data courtesy: TGS, Calgary*)

Energy ratio coherence

$$\text{5. coherence} \equiv \frac{\text{energy of coherent compt}}{\text{energy of input traces}}$$

1. Calculate energy of input traces

2. Calculate the wavelet that best fits the data within the analysis window.

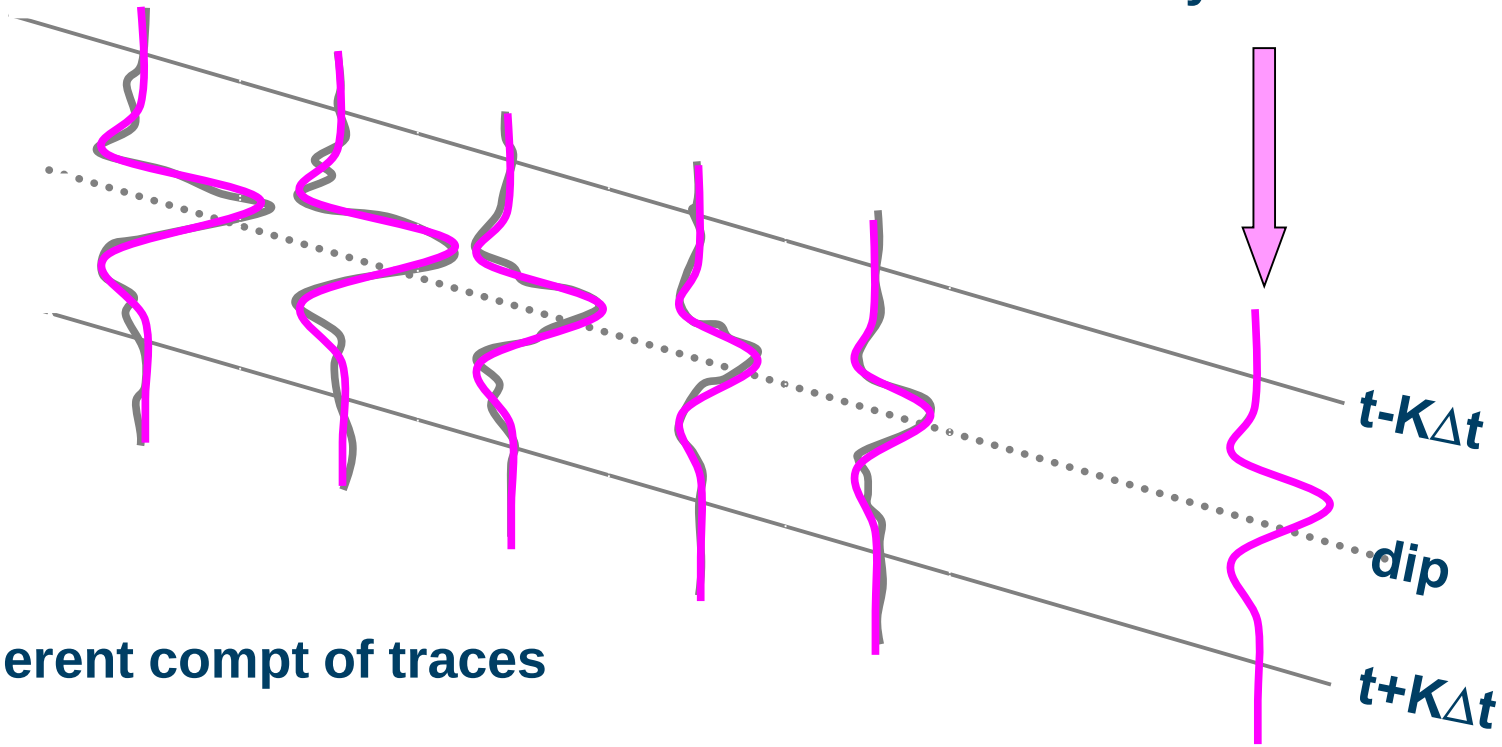

3. Estimate coherent compt of traces

4. Calculate energy of coherent compt of traces

Energy ratio coherence

In the energy ratio algorithm, the covariance matrix is computed from the analytic trace composed of the seismic data, **d**, and its Hilbert transform, $\mathbf{d^H}$, along the structural dip, to prevent structural leakage', corresponding to zero crossings.

$$C_{mn} = \sum_{k=-K}^{K} [d(t_k, x_m, y_m)d(t_k, x_n, y_n) + d^H(t_k, x_m, y_m)d^H(t_k, x_n, y_n)] .$$

$$\mathbf{C}\mathbf{v}^j = \lambda_j \mathbf{v}^{kj} ,$$

where **C** is an *M* by *M* square covariance matrix, λ_j is the j^{th} eigenvalue, and $\mathbf{v}^j$ is the corresponding eigenvector.

The energy ratio coherence is computation is given as:

$$C_{Energy\ ratio} = \frac{\sum_{k=-K}^{+K}\sum_{m=1}^{M}\{[d_{PC}(t_k, x_m, y_m)]^2 + [d_{PC}^H(t_k, x_m, y_m)]^2\}}{\sum_{k=-K}^{+K}\sum_{m=1}^{M}\{[d(t_k, x_m, y_m)]^2 + [d^H(t_k, x_m, y_m)]^2\}} .$$

$$C_{Energy\ ratio} = \frac{E_{coh}}{E_{tot}} .$$

Multispectral energy ratio coherence

Marfurt (2017) constructed a multispectral covariance matrix oriented along structural dip using the analytic voice components, and therefore twice as many sample vectors (i.e. spectral voices and their Hilbert transforms):

$$C_{mn} = \sum_{l=1}^{L} \sum_{k=-K}^{K} [u(t_k, f_l, x_m, y_m) u(t_k, f_l, x_n, y_n) + u^H(t_k, f_l, x_m, y_m) u^H(t_k, f_l, x_n, y_n)] .$$

The corresponding energy ratio coherence computed using this equation is then referred to as *multispectral coherence*.

Multispectral energy ratio coherence applications

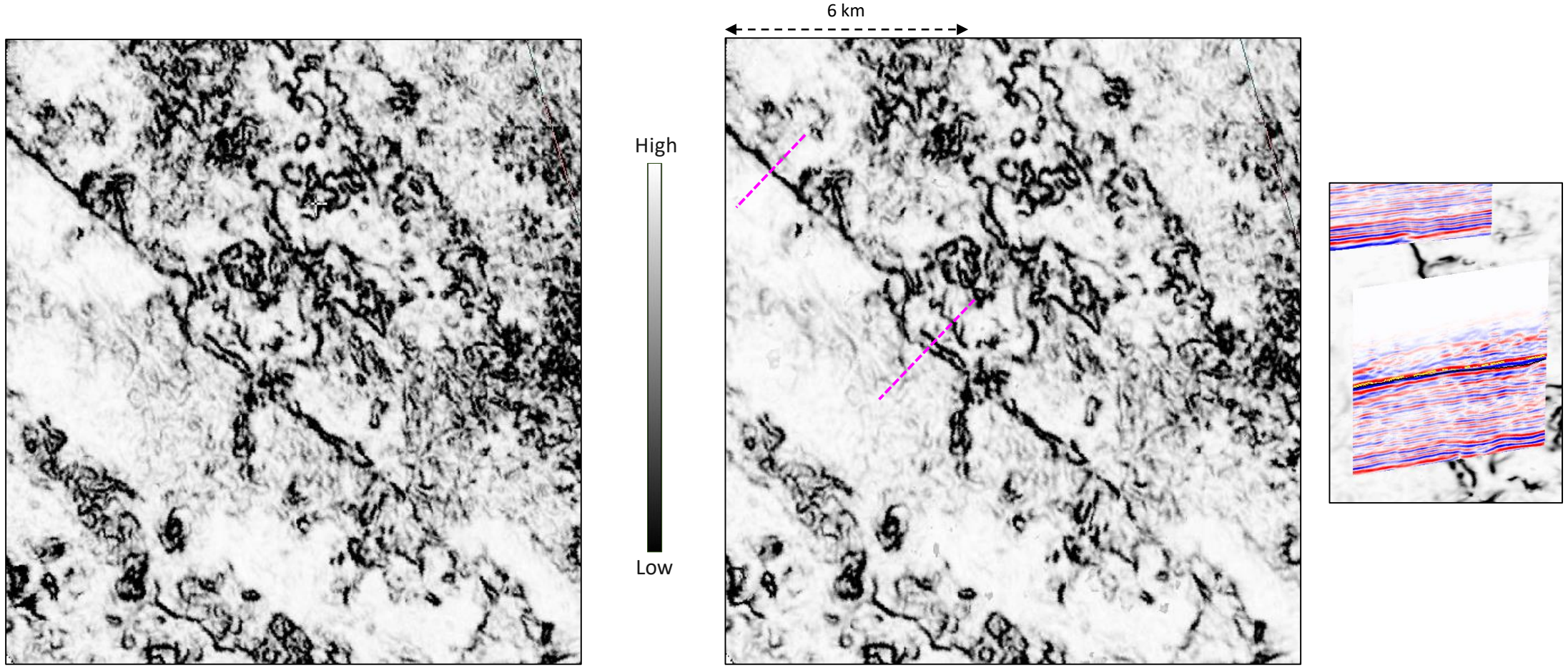

Conventional coherence

Multispectral coherence

Equivalent time slices (664 ms).

The multispectral coherence display depicts clearer and distinct definition of the different features. The seismic data shown is from the Delaware Basin in western Texas. *(Data courtesy of TGS, Houston)*

Multispectral energy ratio coherence applications

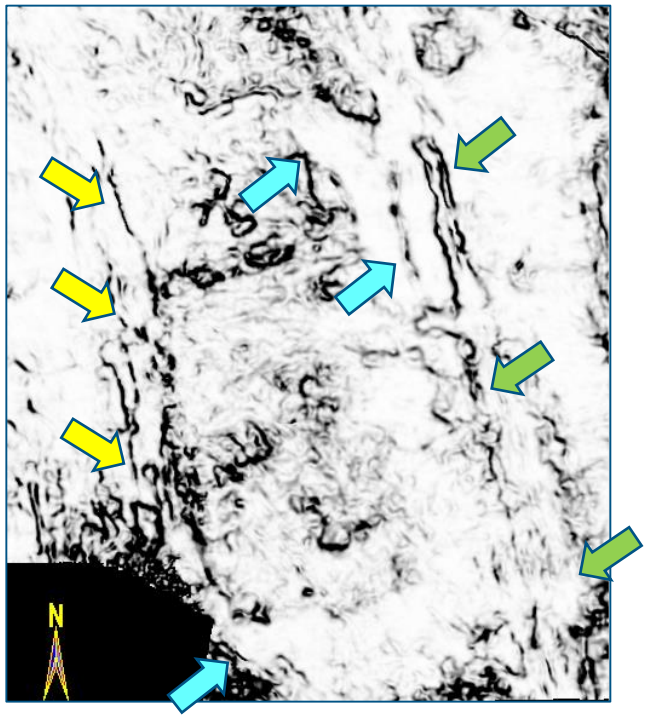

Conventional coherence

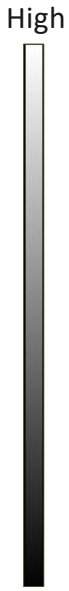

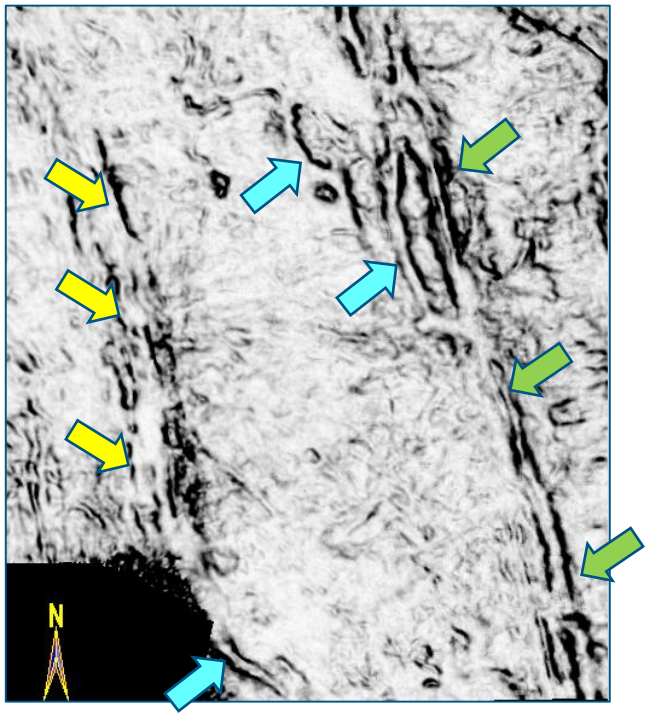

Multispectral coherence

{Generated by using twelve selected voice component (20, 25, 30, 35, 40, 45, 50, 55, 60, 65, 70 and 75 Hz) volumes}

Stratal slices 36ms **above** a marker at roughly 1700ms

Multispectral energy ratio coherence applications

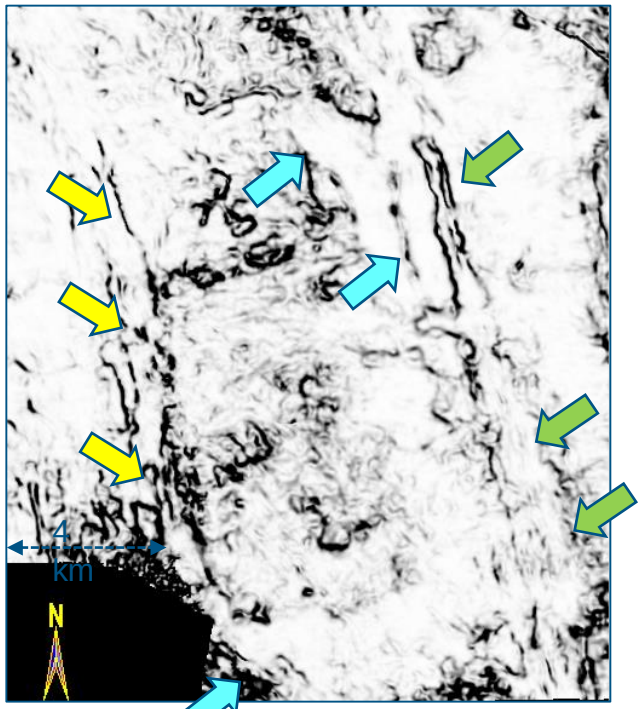

Conventional coherence

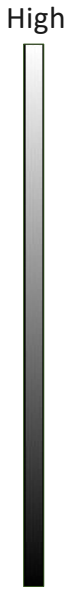

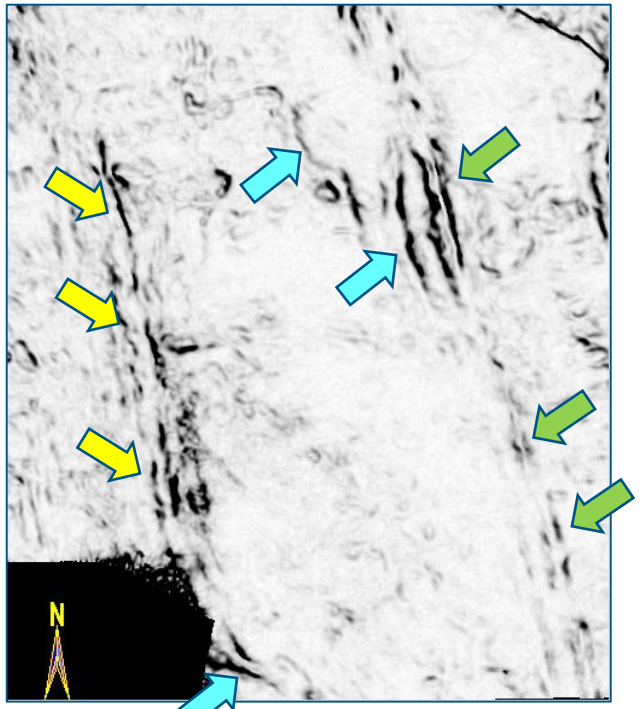

Multispectral coherence

{Generated by using twelve selected voice component (20, 25, 30, 35, 40, 45, 50, 55, 60, 65, 70 and 75 Hz) volumes}

Notice, the overall better definition of faults on the multispectral coherence volume

Stratal slices generated at a marker at roughly 1700ms. The seismic data is from the Montney-Dawson area in British Columbia, Canada. (*Data courtesy: TGS, Calgary)*

Multispectral energy ratio coherence applications

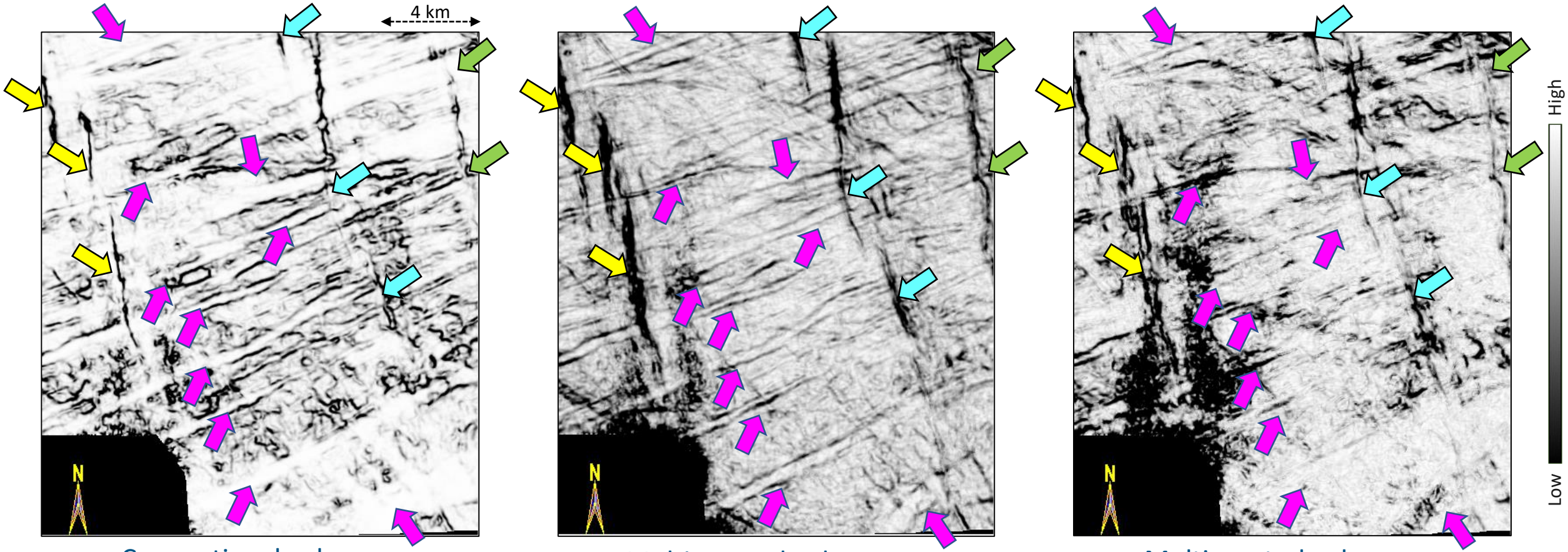

Conventional coherence

Multispectral coherence
{Generated by using twelve selected voice component (20, 25, 30, 35, 40, 45, 50, 55, 60, 65, 70 and 75 Hz) volumes}

Multispectral coherence
{Generated by using six voice component (50, 55, 60, 65, 70 and 75 Hz) volumes}

Stratal slices 38ms above a marker at roughly 1400ms. Notice, the overall better definition of faults (indicated with yellow, cyan and green arrows), and the paleo channels (indicated with purple arrows) on the multispectral coherence volume.

(Data courtesy: TGS, Calgary)

Azimuth-based coherence

Full-azimuth volume

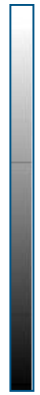

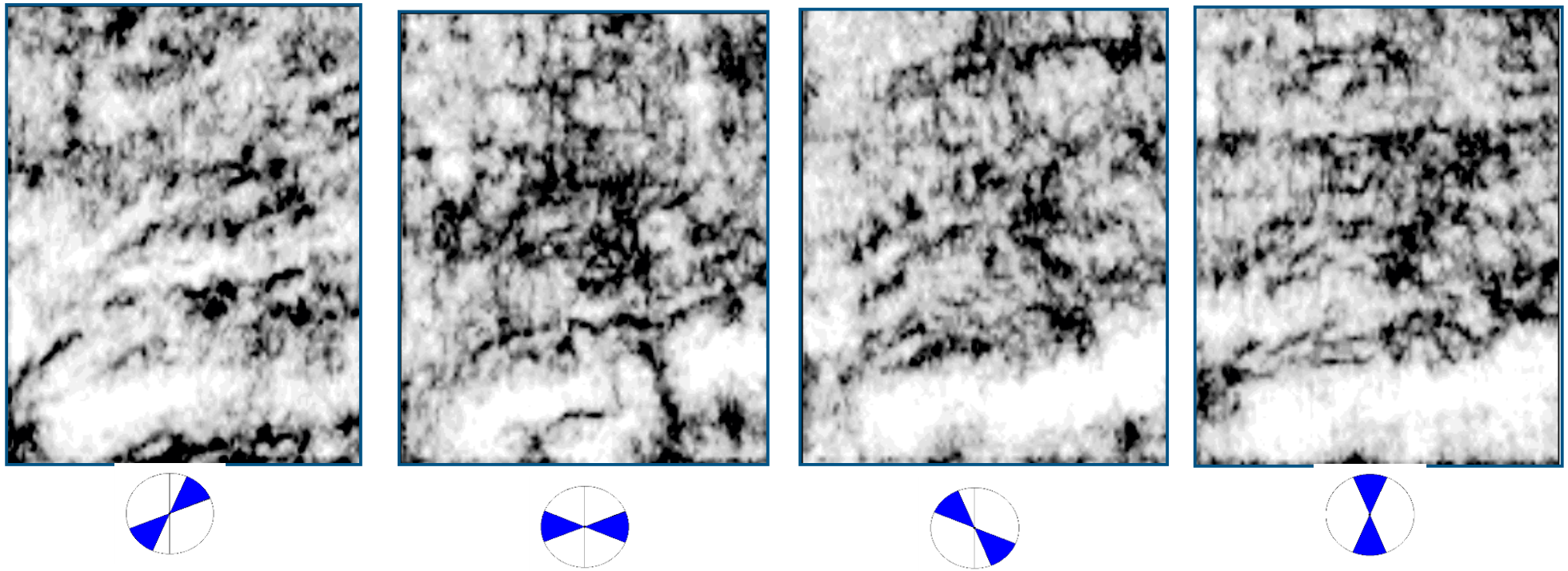

Time slices at 1312 ms through coherence computed from full azimuth and azimuth-limited seismic volumes. Chopra et al.(2000)

Multiazimuth energy ratio coherence

With the focus on shale resource plays, wide azimuth surveys are being commonly being acquired.

Coherence on azimuth-sectored data has been demonstrated before, and though it exhibits better lateral resolution, it is found to be noisy.

Similar to multispectral coherence, the covariance matrix is modified to be the sum of the covariance matrices, each coming from an azimuthally limited volume. The summed covariance matrix to compute the coherent energy (Qi et al., 2017).

This computation is referred to as *multiazimuth* coherence.

$$C_{multi-\varphi} = \sum_{j=i}^{J} \boldsymbol{C}(\varphi_j)$$

The covariance matrix obtained by summation has the same size as the original single-azimuth covariance matrix, but now has J times as many sample vectors.

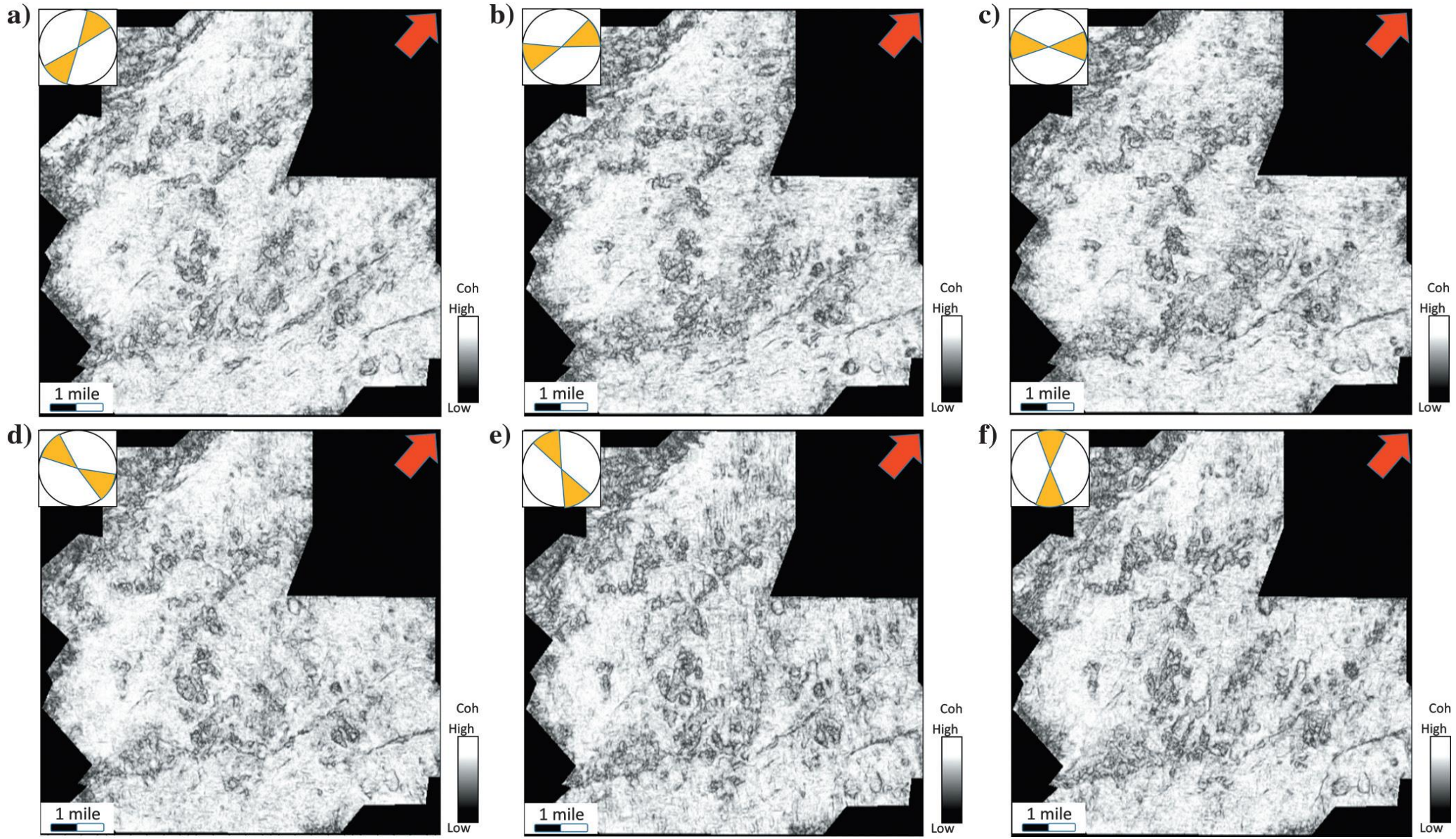

Time slices at 740 ms from coherence volumes computed from azimuthally-limited seismic data. Notice the low S/N ratio as well as the variation in the definition of the karst and fault features. *(Qi et al, 2017)*

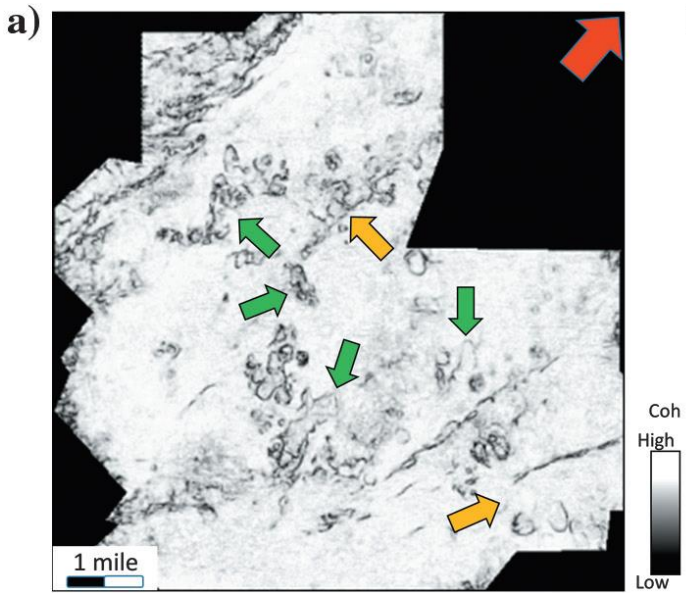

Post-stack seismic data

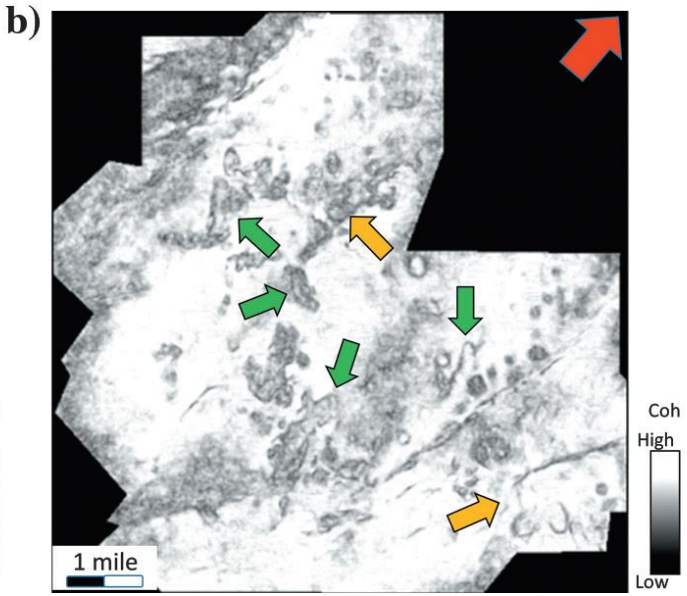

Sum of azimuth-limited coherence slices

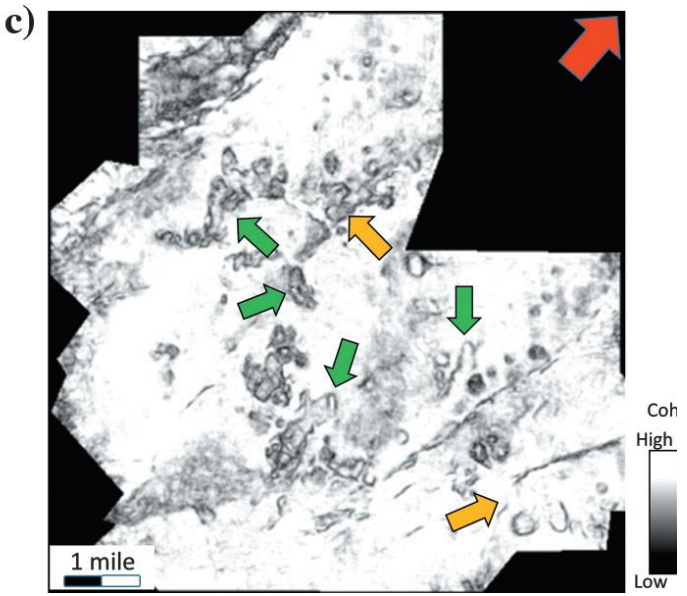

Multi-azimuth coherence

Time slices at 740 ms from coherence volumes computed from azimuthally-limited seismic data. Notice the low S/N ratio as well as the variation in the definition of the features. Seismic data from Fort Worth Basin, Texas. *(Qi et al, 2017)*

Multiazimuth energy ratio coherence

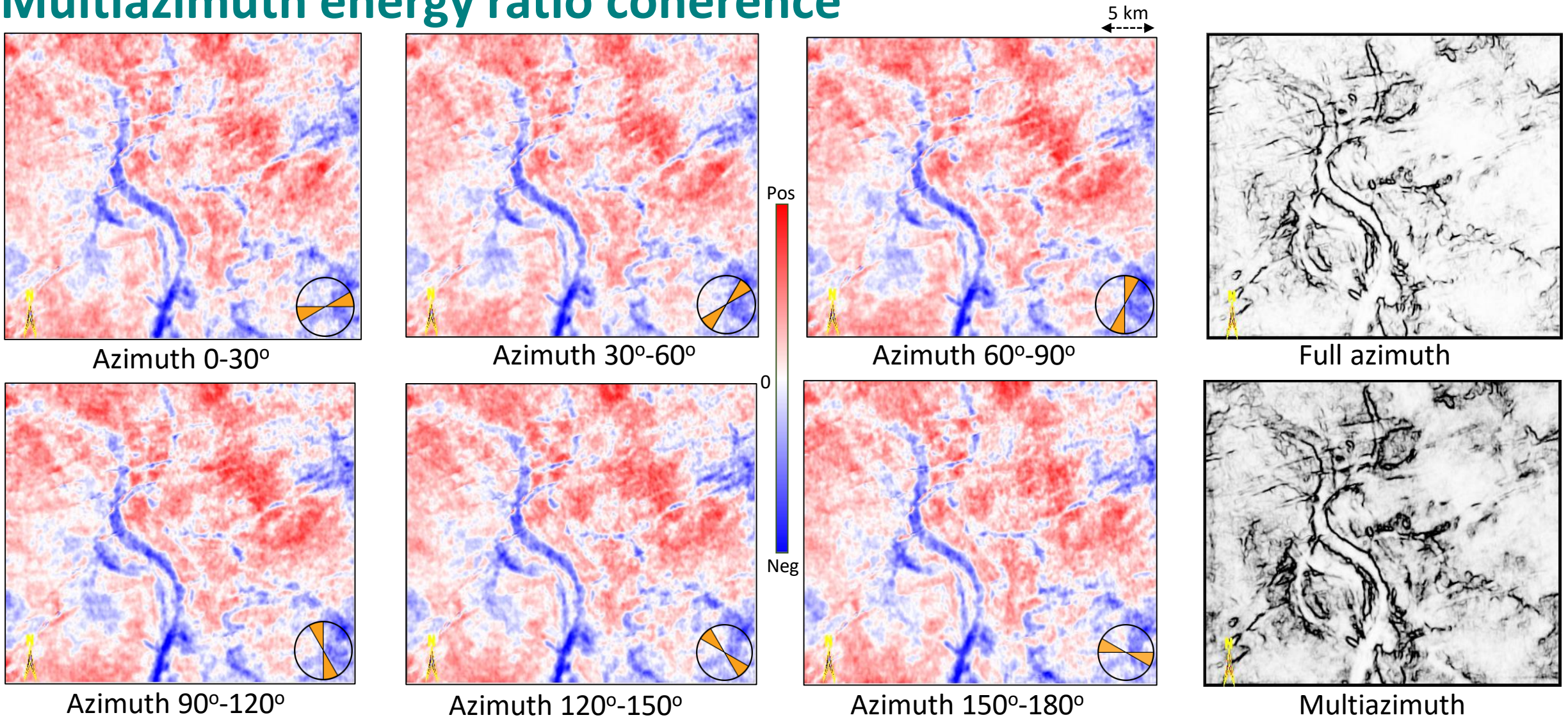

Stratal slices 12ms **above** a marker at roughly 1950ms from different seismic data volumes as indicated. The seismic data is from the STACK trend in Oklahoma. *(Data courtesy: TGS, Houston)*

Multiazimuth energy ratio coherence

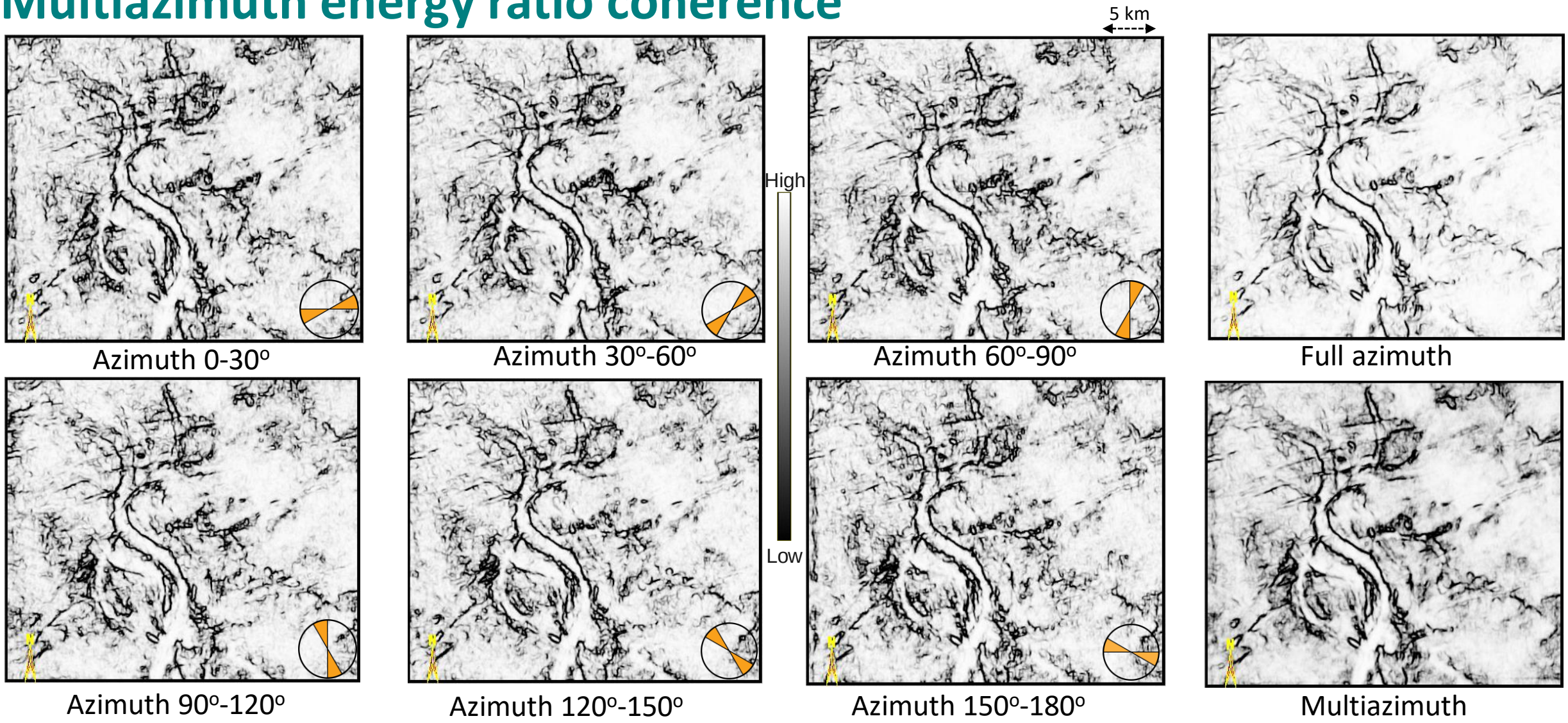

Stratal slices 12ms **above** a marker at roughly 1950ms from different coherence volumes as indicated. The seismic data is from the STACK trend in Oklahoma. *(Data courtesy: TGS, Houston)*

Multiazimuth energy ratio coherence

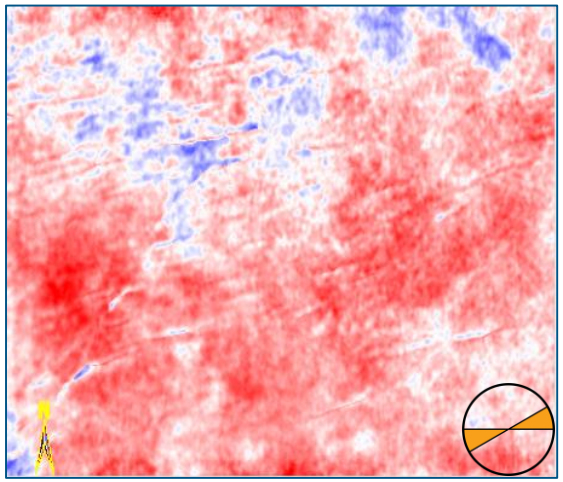

Azimuth 0-30°

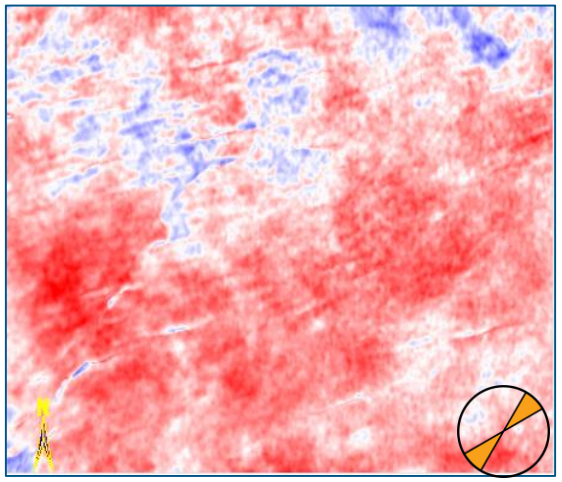

Azimuth 30°-60°

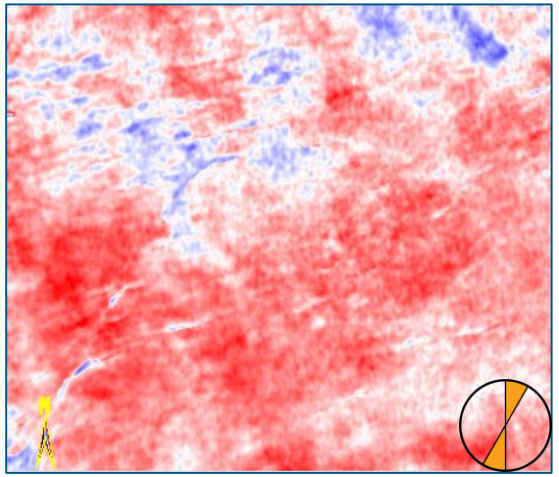

Azimuth 60°-90°

Full azimuth

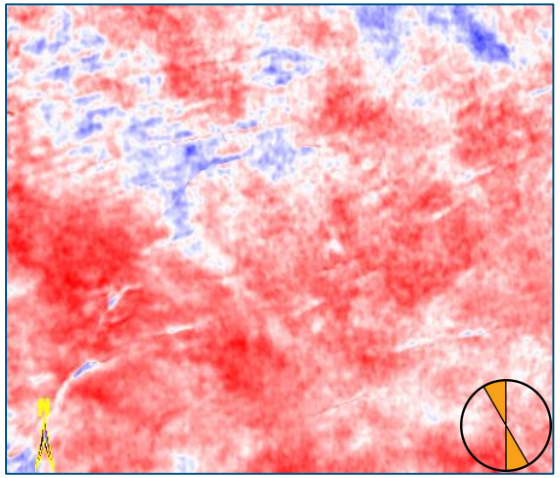

Azimuth 90°-120°

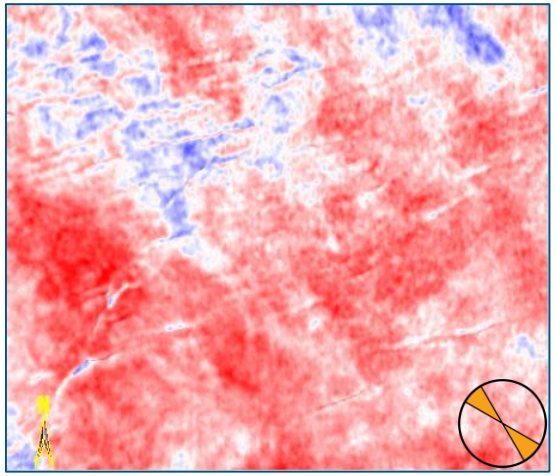

Azimuth 120°-150°

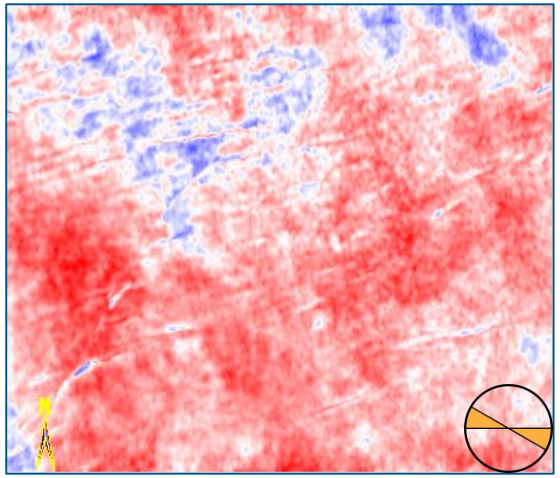

Azimuth 150°-180°

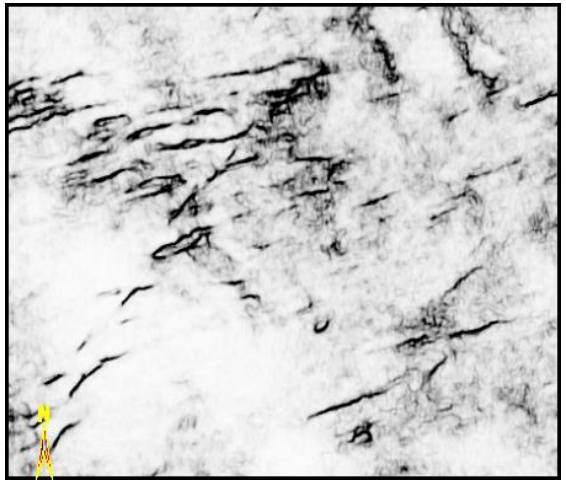

Multiazimuth

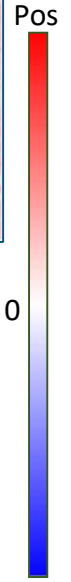

Stratal slices 22ms **below** a marker at roughly 1950ms from different seismic data volumes as indicated. The seismic data is from the STACK trend in Oklahoma. *(Data courtesy: TGS, Houston)*

Multiazimuth energy ratio coherence

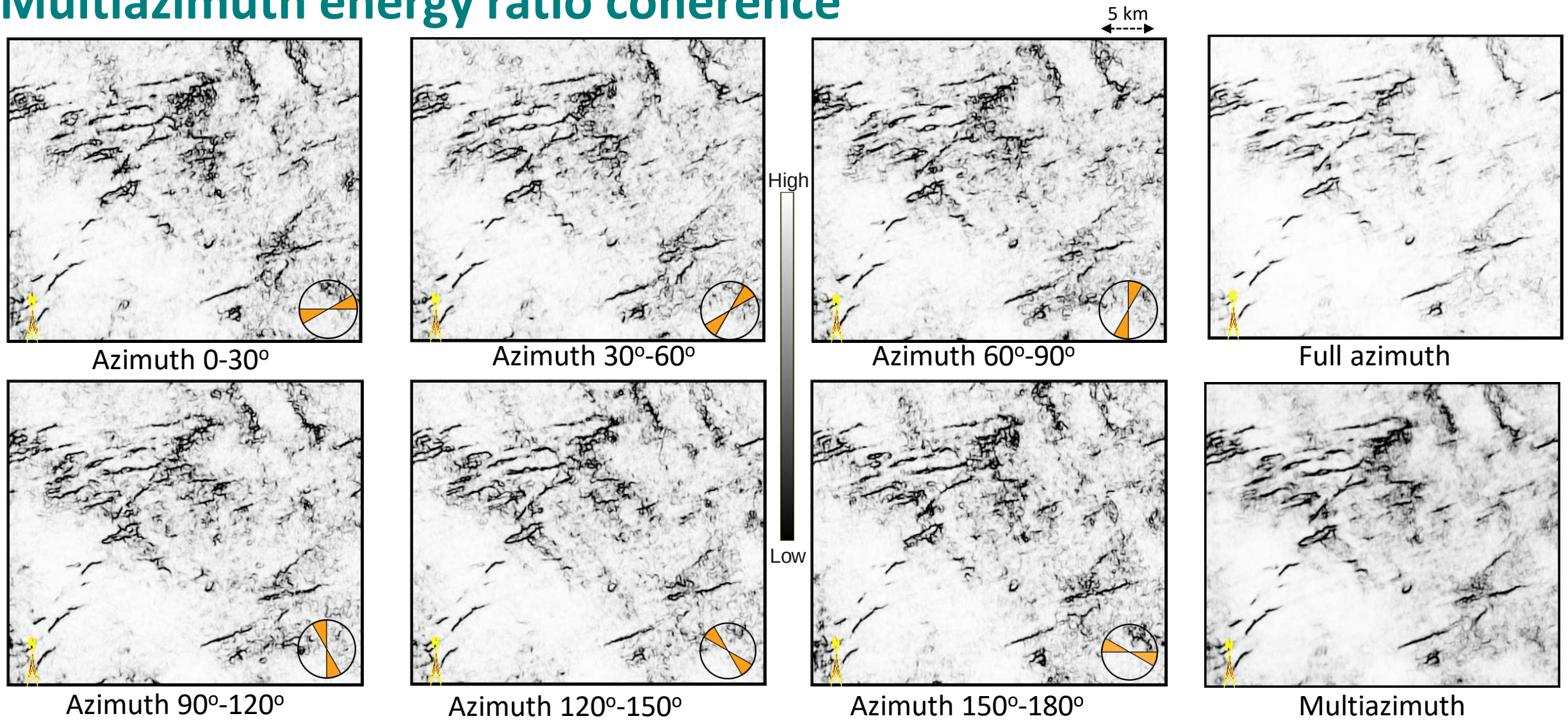

Stratal slices 22ms **below** a marker at roughly 1950ms from different coherence volumes as indicated. The seismic data is from the STACK trend in Oklahoma. *(Data courtesy: TGS, Houston)*

Multioffset energy ratio coherence

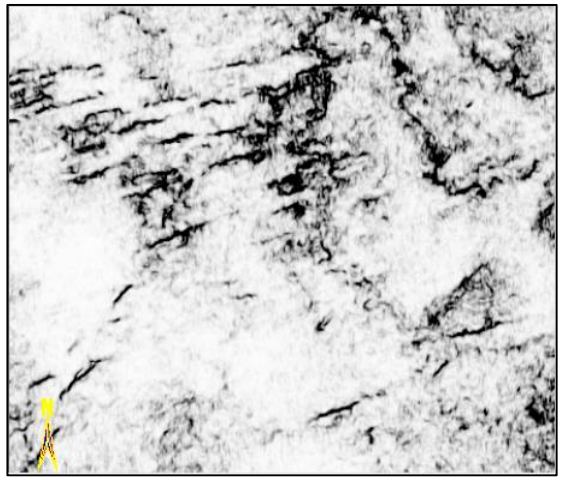

Offset: 0 – 3600 ft

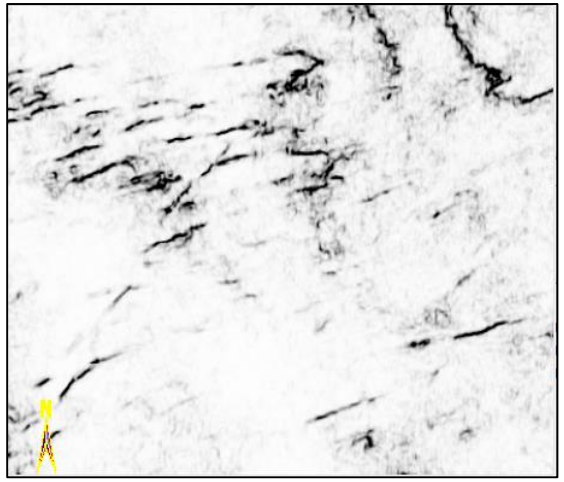

Offset: 3601 – 6800 ft

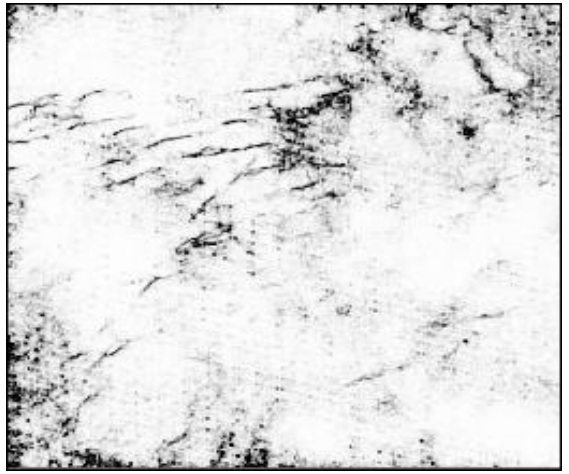

Full offset

5 km

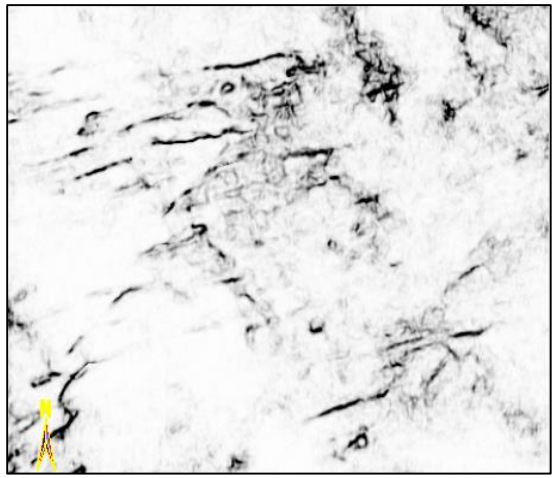

Offset: 6801 -10,200 ft

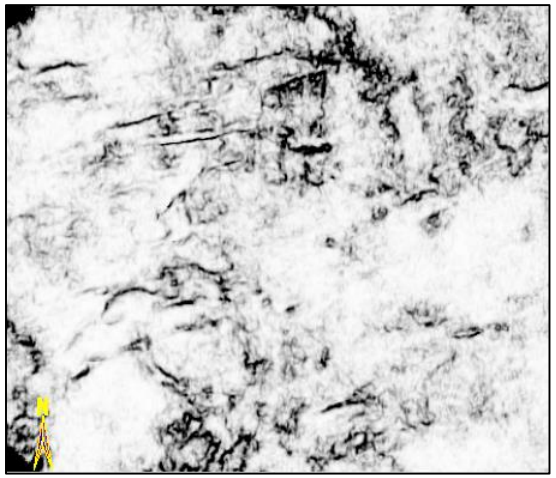

Offset: 10,200 – 13600 ft

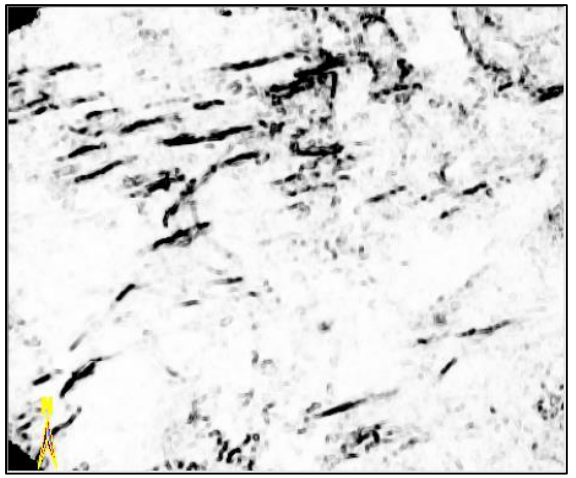

Multioffset

Stratal slices 12ms **above** a marker at roughly 1950ms from different coherence volumes as indicated.

Conclusions

1. Multispectral, multiazimuth and multioffset/angle coherence computations exhibit higher signal-to-noise ratio and higher lateral resolution on the displays.

2. Interpretations carried out on such coherence volumes will be more accurate.

3. Such coherence volumes when used to extract more information by way of fault probability volumes or tools like ant tracking are likely to provide more detailed interpretation.

Acknowledgements

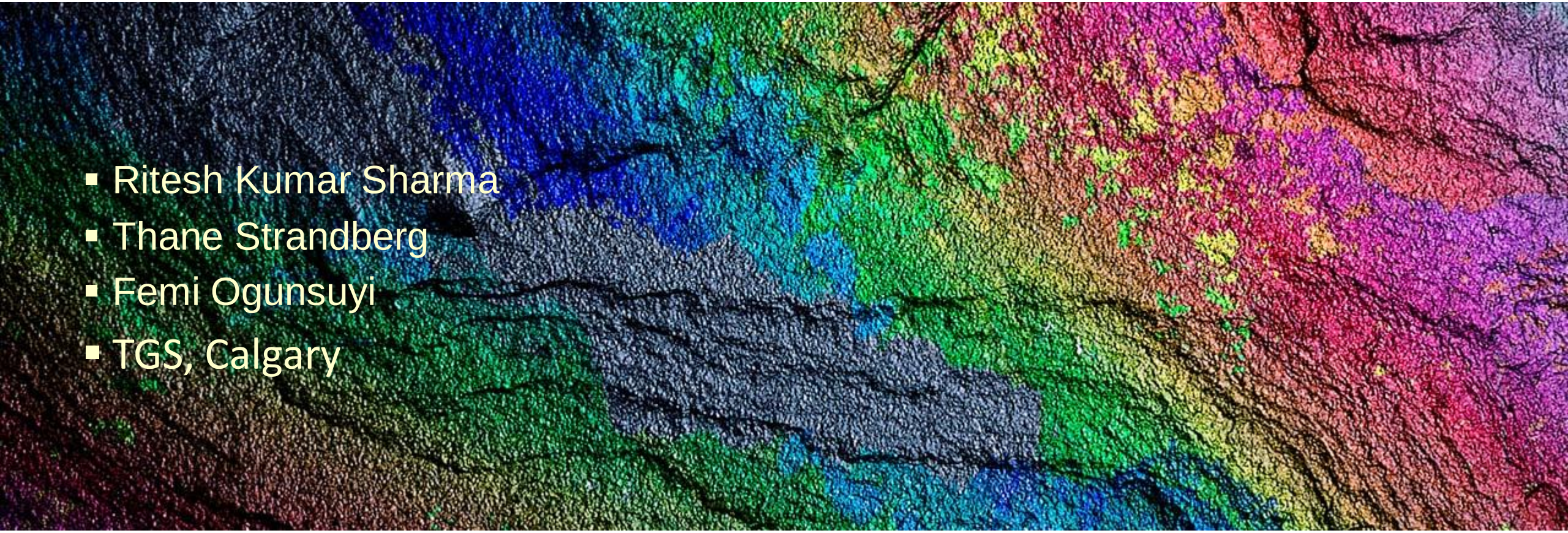

- Ritesh Kumar Sharma
- Thane Strandberg
- Femi Ogunsuyi
- TGS, Calgary